Journal of Computational Mathematics, Vol.23, No.2, 2005, 131–152.

EXPONENTIAL MESH APPROXIMATIONS FOR A 3D EXTERIOR PROBLEM IN MAGNETIC INDUCTION *

Séraphin M. Mefire
(*Laboratoire Amiénois de Mathématique Fondamentale et Appliquée, CNRS UMR 6140, Université de Picardie Jules-Verne, 33 r. Saint-Leu, 80039 Amiens Cedex 1, France*)

Dedicated to the Memory of Doctor E. Nabana

Abstract

A numerical method combining the approaches of C.I. Goldstein and L.-A. Ying is used for the simulation in three-dimensional magnetostatics related to an exterior problem in magnetic induction. Recently introduced, this method is based on the use of a graded mesh obtained by gluing homothetic layers in the exterior domain and has been performed in the case of edge element discretizations. In this work, the theoretical and practical aspects of the method are inspected in the case of face element and volume element discretizations, for computing a magnetic induction. Error estimates, implementations, and numerical results are provided.

Mathematics subject classification: 65N15, 65N30, 65N38, 65R20, 78A30.
Key words: Exterior problems, Magnetostatics, Mixed formulations, Graded meshes, Face elements, Volume elements, Boundary elements, Truncations, Error estimates.

1. Introduction

When we are concerned with the numerical simulation associated with a linear exterior problem, we use in major cases the boundary integral method for discretizing the problem. This approach requires the discretization of boundary integral operators and following the usual processes, we are led to consider dense matrices in computations. Typically, when we compute the magnetic induction (see e.g. [15]) in three-dimensional magnetostatics, we use a vector-valued boundary integral operator with which a dense matrix is associated by finite element techniques. The assembling of such a matrix is not easy, and moreover its size, proportional to the square of the number of boundary edges, can forbid fine meshes for storage requirements.

Goldstein's approach (see [14]) is an alternative to the boundary integral method. This approach is based on the coupling of the finite element method with an appropriately graded mesh near infinity. The original exterior problem is rewritten in a bounded truncated domain for which the boundary is near infinity. The definition of this truncated domain and the use of a graded mesh are crucial in such a way that optimal error estimates hold between the original continuous solution and the discrete solution—resulting from the truncated domain.

In another approach, Ying has introduced in [20] an infinite mesh method for exterior domains. The method is based on a superposition of homothetic layers and therefore provides a kind of graded mesh. The main difference between the boundary integral method and Ying's approach concerns the discretization of boundary integral operators. Namely in the case of the Poincaré-Steklov operator, he builds recursively a sequence of stiffness matrices that converges to the stiffness matrix of the infinite mesh corresponding thus to the discretization of the Poincaré-Steklov operator.

* Received March 24, 2003; final revised August 23, 2004.

Other alternatives to the boundary integral method can be found in [4], [13], [16] as well as in additional references cited therein.

We are concerned here with an approach recently introduced in [1], [2], called the *exponential mesh approximation*, mixing the methods of Goldstein [14] and Ying [20], and which consists of building an infinite mesh as in [20] and of doing truncations of this mesh as in [14]. This method has been applied to the computation of the demagnetizing potential in micromagnetics [1], and to the computation of a magnetic reaction field [2]. The exponential mesh consists of an assembling of homothetic layers in the exterior domain and gives a natural way to get a graded mesh at infinity. Locally in each homothetic layer, finite element approximations are considered. For example, Lagrange's elements are used in [1] and edge elements are used in [2]. Here, we will consider face element and volume element approximations.

The exterior problem considered hereafter comes from magnetostatics and consists of finding a vector field B such that:

$$\operatorname{div} B \;=\; 0 \;\text{ in }\; \mathbb{R}^3 \;\text{ and }\; \operatorname{curl}(\nu\, B) \;=\; J \;\text{ in }\; \mathbb{R}^3\,.$$

The datum J is a current density, B is the magnetic induction, and ν is a physical parameter used to describe the magnetic reluctance of the considered material. In what follows, a magnetic material will typically be represented by a bounded domain Ω with boundary Γ. Also, ν will take in $\Omega' = \mathbb{R}^3 \setminus \overline{\Omega}$ the value ν_0, the reluctance of the vacuum. Time-independent, the current density is considered here as: $J = \widetilde{j}$, the extension, outside Ω by zero, of a vector field j confined to Ω, divergence-free, square integrable with normal trace on Γ equal to zero. In the space, this current density creates a source field h^s: $\operatorname{curl} h^s = J$, $\operatorname{div} h^s = 0$ in $\mathbb{R}^3$, which can be explicitly determined with the help of the Biot-Savart formula [5]. The original system is thus reformulated as a new problem where h^s appears as a datum: find a vector field B such that

$$\operatorname{div} B \;=\; 0 \;\text{ in }\; \mathbb{R}^3\,, \tag{1}$$

$$\operatorname{curl}(\nu\, B) \;=\; \operatorname{curl} h^s \;\text{ in }\; \mathbb{R}^3\,, \tag{2}$$

$$\lim_{|x|\to\infty} |B(x)| \;=\; 0\,.$$

A recent approach (see e.g. [15]) proposed for solving $(1)-(2)$ consists of considering a mixed formulation in which the restriction of B to Ω, used as unknown in Ω, is coupled on Γ with a vector-valued boundary unknown allowing to represent B in Ω' with the help of a vector potential. With such a formulation, which uses of course a vector-valued boundary integral operator, $(1)-(2)$ is treated by a mixed finite element method.

A variational mixed method is also used in our approach in order to solve $(1)-(2)$. Namely, besides B which appears as an unknown in the considered mixed formulation, a scalar field also defined in $\mathbb{R}^3$ is used as an auxiliary unknown. A first difference with the mixed formulation using a boundary integral operator is that B is no longer represented in Ω' with the help of a vector potential. More precisely, our formulation does not use any boundary unknown and we suggest to discretize this formulation with the help of exponential mesh approximations.

This work contains five sections. In section 2 we consider some notations and introduce from $(1)-(2)$ a mixed formulation in magnetic induction.

Exponential mesh approximations are reported in section 3. In this part, we start by describing the discretization of the whole space $\mathbb{R}^3$ with the help of an exponential mesh. Then, we introduce the discrete spaces of infinite dimension in which the unknowns are determined, and consider a discrete formulation on the exponential mesh for which we derive an error estimate. This formulation yields a discrete system of infinite dimension and we truncate the exponential mesh in order to reduce the size of the system to a finite dimension. A second error estimate for the truncated system is established with an asymptotic formula between the interior mesh size, the homothetic coefficient ξ and the number of homothetic layers N considered for the exponential mesh. We consider two kinds of boundary condition on the magnetic induction

when we truncate the exponential mesh; namely a Dirichlet boundary condition and a boundary condition of Neumann type. Two discrete systems, where each system is associated with one kind of boundary condition, are then considered for computations. The matrix of each system is sparse and its condition number depends highly on the two parameters ξ and N. The matrix for the exterior mesh is built with the knowledge of the matrix in the first homothetic layer [20]. Since only the matrix in the first layer is stored for the exterior mesh, saving of memory storage is easily performed. We conclude this section by discussing some algorithms used to solve our systems.

Numerical results deriving from exponential mesh computations are described in section 4 and some conclusions are reported in section 5.

2. Mixed Continuous Formulation

2.1 Some Notations

The usual notation for Sobolev spaces is employed; the scalar product associated with a Hilbert space X is denoted by $(\,.\,,\,.\,)_X$ and the corresponding norm by $\|\,.\,\|_X$. We consider Ω a bounded convex open subset of $\mathbb{R}^3$, with connected boundary Γ. Let $\Omega' = \mathbb{R}^3 \setminus \overline{\Omega}$, and assume that

$$h^s \in \{u \in (L^2(\mathbb{R}^3))^3\,;\ \operatorname{div} u \,=\, 0 \ \text{ in } \ \mathbb{R}^3\,,\ \operatorname{curl} u \,=\, 0 \ \text{ in } \ \Omega'\}\,, \tag{3}$$

$$\nu(x) = \nu_0 > 0 \ \ \forall\, x \in \Omega', \quad 0 < \nu_\star \le \nu(x) < \nu_0 \ \ \forall\, x \in \Omega, \tag{4}$$

where $\nu_\star$ is a real constant.

Let us consider

$$H(\operatorname{div}\,; D) \,=\, \{u \in (L^2(D))^3\,;\ \operatorname{div} u \in L^2(D)\}\,,$$

the Hilbert space endowed with the scalar product (see [11])

$$(u,\eta)_{H(\operatorname{div}\,;\,D)} = (u,\eta)_{(L^2(D))^3} + (\operatorname{div} u, \operatorname{div}\eta)_{L^2(D)}\,,$$

where D can be $\mathbb{R}^3$ or a bounded open subset of $\mathbb{R}^3$. The vector field B satisfying (1) – (2), i.e.

$$\operatorname{div} B \,=\, 0 \ \text{ in } \ \mathbb{R}^3 \ \text{ and } \ \operatorname{curl}(\nu B) \,=\, \operatorname{curl} h^s \ \text{ in } \ \mathbb{R}^3\,,$$

is sought in $\mathfrak{B} \,=\, H(\operatorname{div}\,;\,\mathbb{R}^3)$.

Let us also consider the space (see [9])

$$W^m(\mathcal{O}) = \{\psi;\ (1+|x|^2)^{\frac{|\alpha|-1}{2}}\,\partial^\alpha\psi \,\in L^2(\mathcal{O}) \ \ \forall\, 0 \,\le |\alpha| \le m\ \}\,,$$

where $\mathcal{O}$ can be Ω' or $\mathbb{R}^3$; m is a strictly positive integer, $\alpha = (\alpha_1, \alpha_2, \alpha_3)$ is a multi-index, $x \,=\, (x_1, x_2, x_3)$ is a point in $\mathbb{R}^3$ and $|x| = \sqrt{x_1^2 + x_2^2 + x_3^2}$.

2.2 Mixed Formulation in Magnetic Induction

From (2) let us introduce, according to the Poincaré lemma [9], $\psi \in W^1(\mathbb{R}^3)$ such that:

$$\nu\, B \,=\, \operatorname{grad}\,\psi + h^s \ \text{ in } \ \mathbb{R}^3\,. \tag{5}$$

The introduction of the auxiliary unknown ψ allows us to rewrite the model problem in the form of a mixed formulation. Equation (2) is replaced by (5) which is written in the weak form

$$(\nu\, B, \eta)_{(L^2(\mathbb{R}^3))^3} + (\operatorname{div}\eta, \psi)_{L^2(\mathbb{R}^3)} = (h^s, \eta)_{(L^2(\mathbb{R}^3))^3} \quad \forall\, \eta \in \mathfrak{B},$$

and equation (1) is also considered in the weak form:

$$(\operatorname{div} B, \phi)_{L^2(\mathbb{R}^3)} = 0 \quad \forall\, \phi \in L^2(\mathbb{R}^3)\,.$$

With these two weak equations we introduce the formulation defined as follows.

For h^s and ν satisfying (3) and (4) respectively, find (B, ψ) in the space $\mathfrak{B} \times L^2(\mathbb{R}^3)$ such that:

$$\left\{ \begin{array}{lllll} (\nu\, B, \eta)_{(L^2(\mathbb{R}^3))^3} & + & (\operatorname{div} \eta, \psi)_{L^2(\mathbb{R}^3)} & = & (h^s, \eta)_{(L^2(\mathbb{R}^3))^3} \quad \forall\, \eta \in \mathfrak{B}\,, \\ & & (\operatorname{div} B, \phi)_{L^2(\mathbb{R}^3)} & = & 0 \qquad\qquad \forall\, \phi \in L^2(\mathbb{R}^3)\,. \end{array} \right. \tag{6}$$

The study of the mixed formulation (6) can be performed with the Babuska-Brezzi framework (see [3], [7]). Let us set

$$a(u, \eta) \,=\, (\nu\, u, \eta)_{(L^2(\mathbb{R}^3))^3}\,, \quad b(u, \phi) \,=\, (\operatorname{div} u, \phi)_{L^2(\mathbb{R}^3)}\,,$$

the continuous bilinear forms on $\mathfrak{B} \times \mathfrak{B}$ and $\mathfrak{B} \times L^2(\mathbb{R}^3)$ respectively. Note that $\eta \in \mathfrak{B} \longmapsto (h^s, \eta)_{(L^2(\mathbb{R}^3))^3}$ is a continuous linear form.

We have

Proposition 2.1. *The formulation* (6) *has at least one solution* $(B, \psi) \in \mathfrak{B} \times L^2(\mathbb{R}^3)$ *and* B *is unique.*

Moreover, B *satisfies* $(1) - (2)$ *and there exists a positive constant* $c := C(\nu_\star)$ *such that* $||B||_{\mathfrak{B}} \,\leq\, c\,||h^s||_{(L^2(\mathbb{R}^3))^3}$.

The closed subspace $V \,=\, \{u \,\in\, \mathfrak{B}\,;\; b(u, \phi) \,=\, 0 \quad \forall\, \phi \,\in\, L^2(\mathbb{R}^3)\}$ can also be written as: $V \,=\, \{u \,\in\, \mathfrak{B}\,;\; \operatorname{div} u \,=\, 0 \quad \text{in} \quad \mathbb{R}^3\}$. Using (4), we get $a(u, u) \,\geq\, \nu_\star\, \|u\|^2_{\mathfrak{B}} \quad \forall\; u \,\in\, V$, and then $a(\,\cdot\,,\,\cdot\,)$ is $V-$elliptic. This allows to deduce, following the Babuska-Brezzi theory, that the formulation (6) has at least one solution and that from each solution $(B, \psi) \in \mathfrak{B} \times L^2(\mathbb{R}^3)$, the vector field B is unique.

Let $(B, \psi) \,\in\, \mathfrak{B} \times L^2(\mathbb{R}^3)$ a solution of (6). From the second weak equation of (6), we obtain that B satisfies (1). By setting $\eta \,=\, \operatorname{curl} \varphi$, with $\varphi \in (\mathcal{D}(\mathbb{R}^3))^3$, it follows from the first weak equation of (6) that the relation (2) holds for B. On the other hand, with $\eta = B$ in the first weak equation of (6), we have: $(\nu\, B, B)_{(L^2(\mathbb{R}^3))^3} \,=\, -\,(\operatorname{div} B, \psi)_{L^2(\mathbb{R}^3)} \,+\, (h^s, B)_{(L^2(\mathbb{R}^3))^3}$. Due to the fact that $B \in V$, we deduce by using (4) and the Cauchy-Schwarz inequality that: $\|B\|_{\mathfrak{B}} \,\leq\, \frac{1}{\nu_\star}\, \|h^s\|_{(L^2(\mathbb{R}^3))^3}$.

The formulation (6) allows us to determine the physical unknown B in accordance with $(1) - (2)$.

3. Exponential Mesh Approximations

3.1 Introduction

To discretize the formulation (6), we consider a mesh with homothetic layers for the exterior domain Ω' as explained in Ying [20]. The construction of the exterior mesh requires the bounded domain Ω to be a convex polyhedron.

For the sake of simplicity, we assume that the center of Ω is the origin $O(0, 0, 0)$. We denote by $\xi > 1$ a real constant and define $\Gamma_k := \xi^k\, \Gamma$, for any positive integer k, the convex polyhedron homothetic to Γ with the constant of proportionality ξ^k and center O. We call a *layer* the bounded domain $\mathcal{C}_k$, delimited by two consecutive polyhedra Γ_{k-1} and Γ_k. All the layers are decomposed into tetrahedra in order to obtain the same shape of mesh for each layer (see in Figure 1. a simple example of multi-layer mesh). We obtain in this way a conforming mesh of Ω'. It is important to already notice that at infinity, the tetrahedra of the triangulation become larger and larger. We couple the multi-layer mesh of Ω' with an interior mesh of Ω (which is described in what follows) in order to define a mesh of $\mathbb{R}^3$.

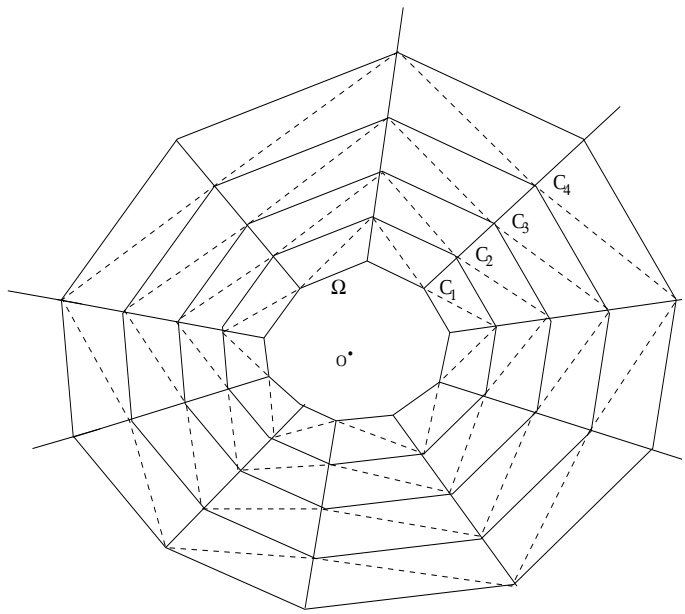

Figure 1: An example of multi-layer mesh outside a bounded domain Ω.

Let us denote by K a tetrahedron, by ϱ_K the diameter of the largest sphere included in K, and by h_K the diameter of K. As usual, we consider a triangulation $\mathcal{T}$ covering Ω and made up of tetrahedra K. The aspect-ratio of $\mathcal{T}$ is defined as follows:

$$h_{\mathcal{T}} \;=\; \sup_{K\in\mathcal{T}} h_K\,.$$

We call $\mathcal{T}_k$ a sequence of triangulations of the convex domain Ω and denote by $\overline{\mathcal{T}}_k$ the triangulation of $\mathbb{R}^3$ obtained by gluing on Γ the triangulation $\mathcal{T}_k$ and the multi-layer triangulation of Ω' described above. We assume that this sequence is regular in the sense that there exists a constant $c > 0$ such that:

$$\forall\, k, \quad \sup_{K\in\mathcal{T}_k\cup\mathcal{C}_1} \frac{h_K}{\varrho_K} \;\le\; c\,,$$

and moreover,

$$\lim_{k\longrightarrow\infty} h_{\mathcal{T}_k\cup\mathcal{C}_1} \;=\; 0\,.$$

It is important to notice that this does imply a dependence of ξ on $h_{\mathcal{T}}$ in the sense that we need to have a triangulation of $\mathcal{C}_1$ as "fine" as $\mathcal{T}_k$. In the sequel, we denote $\mathcal{T}$ instead of $\mathcal{T}_k$ and $\overline{\mathcal{T}}$ instead of $\overline{\mathcal{T}}_k$ when no confusion is possible.

Let P_m be the space of polynomials of degree less than or equal to m, with m a positive integer, and let $\widetilde{P}_m$ be the space of homogeneous polynomials of degree m.

Consider the vectorial subspace (see Raviart & Thomas [19]):

$$D^1 \;=\; (P_0)^3 \oplus P_0\, x\,;\; x = \begin{pmatrix} x_1 \\ x_2 \\ x_3 \end{pmatrix}.$$

We associate with $\mathfrak{B}$ the discrete space:

$$\mathfrak{B}_h \;=\; \{B_h \in \mathfrak{B}\,;\; B_h|_K \in D^1 \quad \forall\, K \in \overline{\mathcal{T}}\}\,.$$

This is an infinite dimensional space since the triangulation $\overline{\mathcal{T}}$ contains an infinite number of tetrahedra. A vector field B_h of the space $\mathfrak{B}_h$ is written in each tetrahedron K as (see e.g. [5], [15]):

$$B_h \;=\; \sum_{f=1}^{4} B_h^f \, 2(\lambda_i \nabla \lambda_j \wedge \nabla \lambda_k + \lambda_j \nabla \lambda_k \wedge \nabla \lambda_i + \lambda_k \nabla \lambda_i \wedge \nabla \lambda_j)\,, \tag{7}$$

where

- f is one of the four faces of K with vertices s^i, s^j, s^k
- B_h^f is the scalar unknown associated with f which represents the flux of B_h on f
- λ_i is the barycentric function associated with the vertex s^i and
- $2(\lambda_i \nabla \lambda_j \wedge \nabla \lambda_k + \lambda_j \nabla \lambda_k \wedge \nabla \lambda_i + \lambda_k \nabla \lambda_i \wedge \nabla \lambda_j)$ is the shape function associated with f.

The space $\mathfrak{B}_h$ is a Hilbert space when endowed with the scalar product of $\mathfrak{B}$.

The discrete space associated with $L^2(\mathbb{R}^3)$ is defined as follows:

$$\mathcal{Q}_h \;=\; \{\psi_h \in L^2(\mathbb{R}^3)\,;\, \psi_h|_K \in P_0 \;\; \forall\, K \in \overline{\mathcal{T}}\}\,.$$

For each $\psi_h \in \mathcal{Q}_h$, the degree of freedom associated with the tetrahedron K is the scalar unknown $\int_K \psi_h \, dx$. The shape function (also called *volume function*) associated with K, and denoted χ_K, is defined such that $\int_K \chi_{K'} \, dx = 1$ if $K = K'$ and $\int_K \chi_{K'} \, dx = 0$ otherwise.

3.2 Discrete Formulation in Magnetic Induction

The discrete formulation associated with (6) is written as follows.

For h^s and ν satisfying (3) and (4), find (B_h, ψ_h) in the space $\mathfrak{B}_h \times \mathcal{Q}_h$ such that:

$$\left\{ \begin{array}{lllll} (\nu\, B_h, \eta_h)_{(L^2(\mathbf{R}^3))^3} & + & (\operatorname{div} \eta_h, \psi_h)_{L^2(\mathbf{R}^3)} & = & (h^s, \eta_h)_{(L^2(\mathbf{R}^3))^3} \quad \forall\, \eta_h \in \mathfrak{B}_h\,, \\ & & (\operatorname{div} B_h, \phi_h)_{L^2(\mathbf{R}^3)} & = & 0 \qquad\qquad\quad \forall\, \phi_h \in \mathcal{Q}_h\,. \end{array} \right. \tag{8}$$

This is a mixed formulation where the physical unknown is the discrete magnetic induction B_h.

As in the continuous case, we introduce

Proposition 3.1. *The formulation* (8) *has at least one solution* $(B_h, \psi_h) \in \mathfrak{B}_h \times \mathcal{Q}_h$ *and the vector field* B_h *is unique and satisfies* (1).

There exists a positive constant $c := C(\nu_\star)$ *such that* $\|B_h\|_{\mathfrak{B}} \;\le\; c\,\|h^s\|_{(L^2(\mathbf{R}^3))^3}$.

Denoting by $V_h \;=\; \{u_h \in \mathfrak{B}_h\,;\; b(u_h, \phi_h) = 0 \;\; \forall\, \phi_h \in \mathcal{Q}_h\}$, a closed subspace of $\mathfrak{B}_h$, we check without difficulty that:

$$V_h \;=\; \{u_h \in \mathfrak{B}_h\,;\;\; \operatorname{div} u_h = 0 \;\text{ in }\; \mathbb{R}^3\}\,.$$

Then, according to (4), we deduce that $a(u_h, u_h) \;\ge\; \nu_\star \, \|u_h\|_{\mathfrak{B}}^2 \;\; \forall\; u_h \in V_h$. This allows to state, following the discrete version of the Babuska-Brezzi theory (see [3], [8], [12]), that the formulation (8) has at least one solution and that, from each solution $(B_h, \psi_h) \in \mathfrak{B}_h \times \mathcal{Q}_h$, the vector field B_h is unique and is an element of V_h. On the other hand, by setting $\eta_h = B_h$ in the first weak equation of (8), it derives that:

$$(\nu\, B_h, B_h)_{(L^2(\mathbf{R}^3))^3} \;=\; -(\operatorname{div} B_h, \psi_h)_{L^2(\mathbf{R}^3)} \;+\; (h^s, B_h)_{(L^2(\mathbf{R}^3))^3}\,.$$

Then, since $B_h \in V_h$, the above relation allows to deduce by using (4) and the Cauchy-Schwarz inequality, the same estimate as in the continuous case: $\|B_h\|_{\mathfrak{B}} \;\le\; \frac{1}{\nu_\star} \, \|h^s\|_{(L^2(\mathbf{R}^3))^3}$.

As before, we note that the formulation (8) allows to determine in a unique way the physical unknown B_h.

3.3 Error Estimates and Truncations

We first establish an error estimate for the exponential mesh between the continuous solution B satisfying (6) and the discrete solution B_h given by (8). We rewrite (8) in a truncated domain in order to consider then a matrix system of finite dimension for the effective numerical calculation of B_h. A second error estimate between B and the discrete solution B_h then computed with the truncated mesh is given. This last error estimate uses an asymptotic formula between the number of layers N, the mesh size of the magnetic domain Ω and the homothetic coefficient ξ.

We will assume in this subsection that ν is more regular: we consider the case

$$\nu(x) = \nu_0 > 0 \ \ \forall\, x \in \Omega', \quad \nu(x) = \nu_1 < \nu_0 \ \ \forall\, x \in \Omega, \tag{9}$$

with $\nu_1 \in \mathbb{R}_+^\star$. This hypothesis is more restrictive than (4).

Remark 3.1. Let h^s and ν be given in (3) and (9). If B satisfies (1) – (2) then, there exists $A \in (W^1(\mathbb{R}^3))^3$ such that: $B = \operatorname{curl} A$ in $\mathbb{R}^3$, and

$$\left\{ \begin{array}{rcl} \operatorname{curl}(\nu_1 \operatorname{curl} A - h^s) & = & 0 \ \text{ in } \ \Omega, \\ \operatorname{curl}(\nu_0 \operatorname{curl} A) & = & 0 \ \text{ in } \ \Omega', \\ [(\nu \operatorname{curl} A - h^s) \wedge n]_\Gamma & = & 0. \end{array} \right. \tag{10}$$

The relation $[(\nu \operatorname{curl} A - h^s) \wedge n]_\Gamma = 0$, where n is the unit normal to Γ, reports the continuity of the tangential trace of $\nu B - h^s$ on Γ provided by (2). In this relation, we denote by $[u]_\Gamma = u|_{\text{ext}\Omega} - u|_{\text{int}\Omega}$ the jump across Γ of an arbitrary field u. The vector field A can be considered as harmonic in Ω', in such a way that by setting

$$p \ = \ \operatorname{curl} A|_{\text{ext}\Omega} \wedge n - \operatorname{curl} A|_{\text{int}\Omega} \wedge n\,, \tag{11}$$

we get in particular the integral representation (see e.g. [6]): $\forall\, x \in \Omega'$,

$$A(x) \ = \ \frac{1}{4\pi} \int_\Gamma \frac{p(y)}{|x-y|}\, d\sigma_y\,. \tag{12}$$

This allows to check in particular that $|\operatorname{curl} A|$ decreases to zero at infinity.

Moreover in this subsection, we replace the hypothesis (3) by the more regular one:

$$h^s \in \{u \in (H^2(\mathbb{R}^3))^3\,;\ \operatorname{div} u \ = \ 0 \ \text{ in } \ \mathbb{R}^3\,,\ \operatorname{curl} u = 0 \ \text{ in } \ \Omega'\,\}\,. \tag{13}$$

In this way, the vector field B has the following regularity: $B|_{\Omega'} \in (W^2(\Omega'))^3$, $B|_\Omega \in (H^2(\Omega))^3$.

In the sequel, we denote by $\mathcal{B}(O,R)$ the open ball of center O and of radius R.

Lemma 3.1. *Let ν and h^s be the data given in* (9), (13), *and $A = (A_1, A_2, A_3)$ satisfying* (10) *with these data and harmonic in Ω'. Let α be a multi-index with $|\alpha| = 2$. There exist $R_\star > 0$ and $C > 0$ such that: $\forall\, x \in \mathbb{R}^3 \setminus \mathcal{B}(O, R_\star)$, $\forall\, 1 \le i \le 3$,*

$$|\partial^\alpha A_i(x)| \ \le \ \frac{C}{|x|^3}\,.$$

Proof. Let us consider A as in (10) and harmonic in Ω'. The hypotheses (9) and (13) provide the regularity of A, $A|_{\Omega'} \in (W^3(\Omega'))^3$, $A|_\Omega \in (H^3(\Omega))^3$ and allow to check from (11) that $p = (p_1, p_2, p_3) \in (L^2(\Gamma))^3$ in particular. We get with the formula (12) that: $\forall\, 1 \le i \le 3$, $\partial^\alpha A_i(x) \ = \ \frac{1}{4\pi} \displaystyle\int_\Gamma p_i(y)\, \partial_x^\alpha (\tfrac{1}{|x-y|})\, d\sigma_y$. On the other hand, since there exists a constant $C > 0$

such that $|\partial_x^\alpha(\frac{1}{|x-y|})| \leq \frac{C}{|x-y|^3}$, it follows that: $|\partial^\alpha A_i(x)| \leq C' \int_\Gamma \frac{|p_i(y)|}{|x-y|^3}\, d\sigma_y$, with $C' > 0$ a constant. The desired estimate is then obtained by using the fact that $p_i \in L^2(\Gamma)$ and by taking any constant $R_\star > 0$ such that $\overline{\Omega} \subset \mathcal{B}(O, R_\star)$.

Remark 3.2. Using the same arguments, we also note that there exist $R_{\star\star} > 0$ and $C > 0$ such that: $\forall\, x \in \mathbb{R}^3 \setminus \mathcal{B}(O, R_{\star\star})$, $\forall\, 1 \leq i \leq 3$, we have $|\partial^\alpha A_i(x)| \leq \frac{C}{|x|^4}$ when $|\alpha| = 3$.

We can now introduce

Theorem 3.1. *Let ν and h^s be given in* (9) *and* (13)*. Let B and B_h satisfying* (6) *and* (8) *respectively. There exists a constant $C > 0$ such that:*

$$\|B - B_h\|_{\mathfrak{B}} \leq C\, h_{\mathcal{T}\cup\mathcal{C}_1}\,.$$

Proof. Let us consider the weak formulations (6) and (8). Since $B \in V = \{u \in \mathfrak{B}\,;\, \operatorname{div} u = 0 \text{ in } \mathbb{R}^3\}$ and $B_h \in V_h = \{u_h \in \mathfrak{B}_h\,;\, \operatorname{div} u_h = 0 \text{ in } \mathbb{R}^3\}$, it follows that: $\forall\, u_h \in V_h$,

$$(\nu\,(B_h - u_h), B_h - u_h)_{(L^2(\mathbb{R}^3))^3} = (\nu\,(B - u_h), B_h - u_h)_{(L^2(\mathbb{R}^3))^3}\,.$$

This allows to check that there exists a constant $C(\nu_\star, \nu_0) > 0$ depending on $\nu_\star$ and ν_0 such that:

$$\|B - B_h\|_{\mathfrak{B}} \leq C(\nu_\star, \nu_0) \inf_{u_h \in V_h} \|B - u_h\|_{\mathfrak{B}}\,. \tag{14}$$

Let us reconsider the face element used to build the discrete space $\mathfrak{B}_h$ and the associated interpolate operator Π_h such that (see e.g. [17]):

$$\|B - \Pi_h B\|_{(L^2(K))^3} \leq c\, h_K\, |B|_{(H^1(K))^3}\,, \quad \|\operatorname{div}(B - \Pi_h B)\|_{L^2(K)} \leq C\, h_K\, |B|_{(H^2(K))^3}\,,$$

where $c, C > 0$ are constants independent of h_K, and $|\,.\,|_{(H^1(K))^3}$, $|\,.\,|_{(H^2(K))^3}$ represent the usual seminorms from $(H^1(K))^3$, $(H^2(K))^3$. With these inequalities, we estimate the right hand side term of (14) following the usual reasoning (see e.g. [12], [17]) and obtain:

$$\|B - B_h\|_{\mathfrak{B}}^2 \leq c_1(\nu_\star, \nu_0) \sum_{K \in \overline{\mathcal{T}}} h_K^2\, (|B|^2_{(H^1(K))^3} + |B|^2_{(H^2(K))^3})\,, \tag{15}$$

where $c_1(\nu_\star, \nu_0) > 0$ is a constant depending on $\nu_\star$, ν_0.

Let us consider the radii $R_\star$, $R_{\star\star}$ given in Lemma 3.1 and Remark 3.2: $\overline{\Omega} \subset \mathcal{B}(O, R)$ with $R = \max(R_\star, R_{\star\star})$, and denote by N the smallest integer such that $\mathcal{B}(O, R) \subset \xi^N\, \Omega$. Setting $d_\star = \min_{x \in \partial\Omega} \operatorname{dist}(O, x)$ and $d^\star = \max_{x \in \partial\Omega} \operatorname{dist}(O, x)$, it follows that:

$$\xi^{N-1}\, d_\star < R < \xi^N\, d^\star\,. \tag{16}$$

Let us now inspect the right hand side term of (15) following the cases where $K \subset \Omega$ and $K \subset \mathcal{C}_n$ with $n \leq N$ or $n > N$.

- If $K \subset \Omega$, it follows without difficulty that

$$\sum_{K \in \mathcal{T}} h_K^2\, (|B|^2_{(H^1(K))^3} + |B|^2_{(H^2(K))^3}) \leq h_{\mathcal{T}}^2\, (|B|^2_{(H^1(\Omega))^3} + |B|^2_{(H^2(\Omega))^3})\,. \tag{17}$$

- If $K \subset \mathcal{C}_n$ with $n \leq N$, then $h_K \leq \xi^{N-1}\, h_{\mathcal{C}_1}$, and with (16) it derives that:

$$h_K \leq \frac{R}{d_\star}\, h_{\mathcal{C}_1} \leq C_\star\, h_{\mathcal{C}_1}\,,$$

where $C_\star > 0$ is a constant independent of N and ξ. Thus,

$$\sum_{K\subset\mathcal{C}_1\cup\mathcal{C}_2\cup\ldots\cup\mathcal{C}_N} h_K^2\,(|B|^2_{(H^1(K))^3}+|B|^2_{(H^2(K))^3})$$
$$\leq C_\star^2\,h_{\mathcal{C}_1}^2\,(|B|^2_{(H^1(\mathcal{C}_1\cup\mathcal{C}_2\cup\ldots\cup\mathcal{C}_N))^3}+|B|^2_{(H^2(\mathcal{C}_1\cup\mathcal{C}_2\cup\ldots\cup\mathcal{C}_N))^3})\,,$$

and therefore

$$\sum_{K\subset\mathcal{C}_1\cup\mathcal{C}_2\cup\ldots\cup\mathcal{C}_N} h_K^2\,(|B|^2_{(H^1(K))^3}+|B|^2_{(H^2(K))^3})\leq C_\star^2\,h_{\mathcal{C}_1}^2\,(\|B\|^2_{(W^1(\Omega'))^3}+\|B\|^2_{(W^2(\Omega'))^3})\,. \tag{18}$$

- If $K\subset\mathcal{C}_n$ with $n>N$,

$$\sum_{K\subset\mathcal{C}_n} h_K^2\,(|B|^2_{(H^1(K))^3}+|B|^2_{(H^2(K))^3})\leq \xi^{2(n-1)}\,(|B|^2_{(H^1(\mathcal{C}_n))^3}+|B|^2_{(H^2(\mathcal{C}_n))^3})\,h_{\mathcal{C}_1}^2\,.$$

Since $B\in V$, we get on the other hand from Lemma 3.1: $|B|^2_{(H^1(\mathcal{C}_n))^3}=|\operatorname{curl}A|^2_{(H^1(\mathcal{C}_n))^3}\leq C\int_{\mathcal{C}_n}\frac{1}{|x|^6}\,dx$, where $C>0$ is a constant, and A satisfies (10). As $x\in\mathcal{C}_n$, we have $|x|\geq\xi^{n-1}\,d_\star$, and therefore $|\operatorname{curl}A|^2_{(H^1(\mathcal{C}_n))^3}\leq C(d_\star,\mathrm{vol}(\Omega))\,\xi^3(\xi^3-1)\xi^{-3n}$, with $C(d_\star,\mathrm{vol}(\Omega))>0$ a constant depending on $d_\star$ and $\mathrm{vol}(\Omega)$. In the same way, we obtain with Remark 3.2 that: $|B|^2_{(H^2(\mathcal{C}_n))^3}=|\operatorname{curl}A|^2_{(H^2(\mathcal{C}_n))^3}\leq c(d_\star,\mathrm{vol}(\Omega))\,\xi^5(\xi^3-1)\xi^{-5n}$, with $c(d_\star,\mathrm{vol}(\Omega))>0$ a constant depending on $d_\star$ and $\mathrm{vol}(\Omega)$. Thus,

$$\sum_{n>N}\sum_{K\subset\mathcal{C}_n} h_K^2\,(|B|^2_{(H^1(K))^3}+|B|^2_{(H^2(K))^3})$$
$$\leq C(d_\star,\mathrm{vol}(\Omega))\,[\xi(\xi^3-1)\sum_{n>N}\xi^{-n}+\xi^3(\xi^3-1)\sum_{n>N}\xi^{-3n}]\,h_{\mathcal{C}_1}^2\,,$$

and therefore

$$\sum_{n>N}\sum_{K\subset\mathcal{C}_n} h_K^2\,(|B|^2_{(H^1(K))^3}+|B|^2_{(H^2(K))^3})\;\leq\;C'(d_\star,\mathrm{vol}(\Omega))\,h_{\mathcal{C}_1}^2\,, \tag{19}$$

with $C'(d_\star,\mathrm{vol}(\Omega))>0$ a constant depending on $d_\star$ and $\mathrm{vol}(\Omega)$.

The desired estimate is then obtained with (17), (18) and (19).

The discrete formulation (8) will not be used directly for effective numerical calculations. Indeed, (8) is set in an unbounded domain and therefore provides a linear system of infinite dimension. As for approximations of exterior problems by truncations (see e.g. [4], [13], [16]), we propose to reformulate (8) in a bounded domain

$$\Omega_N\;=\;\xi^N\,\Omega\,,$$

which is the union of the magnetic domain Ω and the N first homothetic layers of the exterior domain Ω'. Typically Ω_N appears here as a truncated domain of the whole three-dimensional space. The reformulation of (8) in Ω_N enforces the use of boundary conditions (see e.g. [16]), on Γ_N the boundary of Ω_N, and allows to consider a linear system of finite dimension for calculations. In what follows, we consider a homogeneous Dirichlet boundary condition and a boundary condition of Neumann type.

3.3.1 Truncation with Dirichlet Boundary Condition

The truncated problem associated with $(1)-(2)$, and using a homogeneous Dirichlet boundary condition, consists of finding a vector field B^N such that:

$$\left\{\begin{array}{rcll} \operatorname{div} B^N & = & 0 & \text{in} \quad \Omega_N\,, \\ \operatorname{curl}(\nu B^N - h^s) & = & 0 & \text{in} \quad \Omega_N\,, \\ B^N \cdot n & = & 0 & \text{on} \quad \Gamma_N\ . \end{array}\right. \tag{20}$$

Here n represents the unit normal to Γ_N outwardly directed to Ω_N.

The discrete formulation associated with (20) consists of finding $(B_h, \psi_h) \in \mathfrak{B}_h^N \times \mathcal{Q}_h^N$ such that:

$$\left\{\begin{array}{rcrcll} (\nu\, B_h, \eta_h)_{(L^2(\Omega_N))^3} & + & (\operatorname{div} \eta_h, \psi_h)_{L^2(\Omega_N)} & = & (h^s, \eta_h)_{(L^2(\Omega_N))^3} & \forall\, \eta_h \in \mathfrak{B}_h^N\,, \\ & & (\operatorname{div} B_h, \phi_h)_{L^2(\Omega_N)} & = & 0 & \forall\, \phi_h \in \mathcal{Q}_h^N\,. \end{array}\right. \tag{21}$$

This is a mixed formulation deriving from (8) where

$$\begin{array}{rcl} \mathfrak{B}_h^N & = & \{u_h \in H(\operatorname{div}\,;\, \Omega_N)\,;\ u_h|_K \in D^1\ \ \forall\, K \in \mathcal{T} \cup \mathcal{C}_1 \cup \cdots \cup \mathcal{C}_N\,, u_h \cdot n = 0\ \text{ on }\ \Gamma_N\,\}, \\ \mathcal{Q}_h^N & = & \{\phi_h \in L^2(\Omega_N)\,;\ \phi_h|_K \in P_0\ \ \forall\, K \in \mathcal{T} \cup \mathcal{C}_1 \cup \cdots \cup \mathcal{C}_N\,\}\,. \end{array}$$

Since

$$\begin{array}{rcl} (u_h, \eta_h) \in \mathfrak{B}_h^N \times \mathfrak{B}_h^N & \longmapsto & (\nu\, u_h, \eta_h)_{(L^2(\Omega_N))^3}\,, \\ (u_h, \phi_h) \in \mathfrak{B}_h^N \times \mathcal{Q}_h^N & \longmapsto & (\operatorname{div} u_h, \phi_h)_{L^2(\Omega_N)}\,, \\ \eta_h \in \mathfrak{B}_h^N & \longmapsto & (h^s, \eta_h)_{(L^2(\Omega_N))^3}\,, \end{array}$$

are continuous and

$$(u_h, \eta_h) \in \mathfrak{B}_h^N \times \mathfrak{B}_h^N \quad \longmapsto \quad (\nu\, u_h, \eta_h)_{(L^2(\Omega_N))^3}$$

is coercitive on

$$V_h^N = \{u_h \in \mathfrak{B}_h^N\,;\ (\operatorname{div} u_h, \phi_h)_{L^2(\Omega_N)} = 0\ \ \forall\, \phi_h \in \mathcal{Q}_h^N\,\} = \{u_h \in \mathfrak{B}_h^N\,;\ \operatorname{div} u_h = 0\ \text{ in }\ \Omega_N\,\}\,,$$

it follows with the usual reasoning (see e.g. [3], [7], [8]) that the truncated discrete formulation (21) has at least one solution $(B_h, \psi_h) \in \mathfrak{B}_h^N \times \mathcal{Q}_h^N$ and that B_h is unique and is an element of V_h^N.

While Ω_N is specified and therefore N is explicitly considered, (21) is suitable for a practical implementation.

3.3.2 Truncation with a Boundary Condition of Neumann Type

The truncated problem associated with $(1)-(2)$, where a boundary condition of Neumann type is enforced, consists of finding a vector field B^N such that:

$$\left\{\begin{array}{rcll} \operatorname{div} B^N & = & 0 & \text{in} \quad \Omega_N\,, \\ \operatorname{curl}(\nu B^N - h^s) & = & 0 & \text{in} \quad \Omega_N\,, \\ (\nu B^N - h^s) \wedge n & = & 0 & \text{on} \quad \Gamma_N\,. \end{array}\right. \tag{22}$$

The discrete formulation associated with (22) consists of finding $(B_h, \psi_h) \in \mathfrak{B}_h^N \times \mathcal{Q}_h^N$ such that:

$$\left\{\begin{array}{rcrcll} (\nu\, B_h, \eta_h)_{(L^2(\Omega_N))^3} & + & (\operatorname{div} \eta_h, \psi_h)_{L^2(\Omega_N)} & = & (h^s, \eta_h)_{(L^2(\Omega_N))^3} & \forall\, \eta_h \in \mathfrak{B}_h^N\,, \\ & & (\operatorname{div} B_h, \phi_h)_{L^2(\Omega_N)} & = & 0 & \forall\, \phi_h \in \mathcal{Q}_h^N\,. \end{array}\right. \tag{23}$$

This is a mixed formulation deriving from (8) where

$$\mathfrak{B}_h^N \;=\; \{u_h \in H(\mathrm{div}\,;\,\Omega_N)\,;\; u_h|_K \in D^1 \;\; \forall\, K \in \mathcal{T} \cup \mathcal{C}_1 \cup \cdots \cup \mathcal{C}_N\,\}\,,$$

and $\mathcal{Q}_h^N$ is defined as previously. The formulation (23) has at least one solution $(B_h, \psi_h) \in \mathfrak{B}_h^N \times \mathcal{Q}_h^N$, and moreover B_h is unique and belongs to

$$V_h^N \;=\; \{u_h \in \mathfrak{B}_h^N\,;\; (\mathrm{div}\, u_h, \phi_h)_{L^2(\Omega_N)} \;=\; 0 \;\; \forall\, \phi_h \in \mathcal{Q}_h^N\,\} \;=\; \{u_h \in \mathfrak{B}_h^N\,;\; \mathrm{div}\, u_h \;=\; 0 \;\text{ in }\; \Omega_N\,\}\,.$$

Contrarily to (8), while N is explicitly determined, the discrete formulation (23) is suitable for a practical implementation since it is set in a bounded domain.

We give below an error estimate between B satisfying (6) and the discrete solution B_h determined with (23). This error estimate allows us to specify the choice of N the number of homothetic layers.

Theorem 3.2. *Let ν and h^s be given in* (9) *and* (13)*. In addition, assume that there exist $R_s > 0$, $C_s > 0$ such that: $\forall\; |x| > R_s$, $|h^s(x)| \leq \frac{C_s}{|x|^2}$. Let B satisfying* (6)*. Consider the number of layers N varying asymptotically according to $h := h_{\mathcal{T}\cup\mathcal{C}_1}$ as follows:*

$$N \sim_{(h \longrightarrow 0)} \; -\,\frac{2\log h}{\log \xi}\,, \tag{24}$$

and B_h satisfying (23)*. Then, there exists a constant $C > 0$ independent of h, N and ξ, such that:*

$$\|B - B_h\|_{H(\mathrm{div}\,;\,\Omega_N)} \;\leq\; C\,h\,.$$

Proof. Let us consider the spaces (see e.g. [17]):

$$\begin{aligned} S^1 \;&=\; \{u \in (\widetilde{P_1})^3\,;\; u \cdot x = 0\}, \quad R^1 = (P_0)^3 \oplus S^1, \\ H(\mathrm{curl};\,\Omega_N) \;&=\; \{u \in (L^2(\Omega_N))^3\,;\; \mathrm{curl} u \in (L^2(\Omega_N))^3\}, \\ \mathcal{H}_h^N \;&=\; \{u_h \in H(\mathrm{curl};\,\Omega_N)\,;\; u_h|_K \in R^1 \;\; \forall\, K \in \mathcal{T} \cup \mathcal{C}_1 \cup \cdots \cup \mathcal{C}_N\,\}. \end{aligned}$$

Let B and B_h satisfying the formulations (6) and (23) associated with (1) – (2) and (22) respectively. Let $A_h \in \mathcal{H}_h^N$ and set $\eta_h = \mathrm{curl} A_h \in V_h^N = \{u_h \in \mathfrak{B}_h^N\,;\; \mathrm{div}\, u_h \;=\; 0 \;\text{ in }\; \Omega_N\,\}$. Using A_h as a test-function and integrating (2) and (22) on Ω_N respectively, it follows that:

$$\int_{\Omega_N} \nu\, B \cdot \eta_h\, dx \;=\; \int_{\Omega_N} h^s \cdot \eta_h\, dx \;+\; \int_{\Gamma_N} (\nu B - h^s) \wedge n \cdot A_h\, d\sigma\,, \tag{25}$$

$$\int_{\Omega_N} \nu\, B_h \cdot \eta_h\, dx \;=\; \int_{\Omega_N} h^s \cdot \eta_h\, dx\,. \tag{26}$$

Following [18], let us consider also the vector field u satisfying:

$$\mathrm{curl} u \;=\; \mathrm{curl} A_h \;\text{ in }\; \Omega_N\,, \quad \mathrm{div} u \;=\; 0 \;\text{ in }\; \Omega_N\,, \quad u \cdot n \;=\; 0 \;\text{ on }\; \Gamma_N\,, \tag{27}$$

and such that,

$$\|u\|_{(H^1(\Omega_N))^3} \leq C_N \|\,\mathrm{curl} A_h\|_{(L^2(\Omega_N))^3}\,, \tag{28}$$

where $C_N > 0$ is a constant depending on N. Since $\mathrm{curl} u = \mathrm{curl} A_h = \eta_h$ in Ω_N, we also obtain by integrating (2) on Ω_N:

$$\int_{\Gamma_N} (\nu B - h^s) \wedge n \cdot A_h\, d\sigma \;=\; \int_{\Gamma_N} (\nu B - h^s) \wedge n \cdot u\, d\sigma\,. \tag{29}$$

Now, let us set $B_h = \mathrm{curl} w_h$, $v_h = \mathrm{curl}\theta_h$, $\eta_h = \mathrm{curl}(w_h - \theta_h)$ with w_h, $\theta_h \in \mathcal{H}_h^N$. It derives from (25) and (26) that:

$$\int_{\Omega_N} \nu\,(B_h - v_h)\cdot(B_h - v_h)\,dx \;=\; \int_{\Omega_N} \nu\,(B - v_h)\cdot(B_h - v_h)\,dx - \int_{\Gamma_N} (\nu\,B - h^s)\wedge n\cdot(w_h - \theta_h)\,d\sigma\,.$$

Using then the same arguments as in (27) – (29), we get that:

$$\int_{\Omega_N} \nu\,(B_h - v_h)\cdot(B_h - v_h)\,dx \;=\; \int_{\Omega_N} \nu\,(B - v_h)\cdot(B_h - v_h)\,dx - \int_{\Gamma_N} (\nu\,B - h^s)\wedge n\cdot(w - \theta)\,d\sigma\,. \quad (30)$$

Of course, (27) and (28) are here considered with $A_h := w_h - \theta_h$, and $u := w - \theta \in (H^1(\Omega_N))^3$. By using then (9) and the Cauchy-Schwarz inequality, we obtain from (30) that:

$$\nu_\star\,\|B_h - v_h\|^2_{(L^2(\Omega_N))^3} \;\le\; \nu_0\,\|B - v_h\|_{(L^2(\Omega_N))^3}\|B_h - v_h\|_{(L^2(\Omega_N))^3} + |\int_{\Gamma_N} (\nu\,B - h^s)\wedge n\cdot(w - \theta)\,d\sigma|\,. \quad (31)$$

The regularity of ν with those of B and h^s allow to estimate the second term of the right hand side of (31) as follows:

$$|\int_{\Gamma_N} (\nu\,B - h^s)\wedge n\cdot(w - \theta)\,d\sigma| \;\le\; \|(\nu\,B - h^s)\wedge n\|_{(L^2(\Gamma_N))^3}\|w - \theta\|_{(L^2(\Gamma_N))^3}\,.$$

The estimate (28) provides therefore here: $\|w - \theta\|_{(L^2(\Gamma_N))^3} \;\le\; c_N\,\|\,\mathrm{curl} w_h - \mathrm{curl}\theta_h\|_{(L^2(\Omega_N))^3}$, with $c_N > 0$ a constant depending on N. Then, by using a dimensional argument, we check that this inequality scales with the homothetic coefficient ξ and becomes:

$$\|w - \theta\|_{(L^2(\Gamma_N))^3} \;\le\; c\,\xi^{\frac{N}{2}}\,\|\,\mathrm{curl} w_h - \mathrm{curl}\theta_h\|_{(L^2(\Omega_N))^3}\,,$$

with $c > 0$ a constant depending only on the shape of Ω. It derives then from (31) that:

$$\|B_h - v_h\|_{(L^2(\Omega_N))^3} \;\le\; c(\nu_0, \nu_\star)\,\|B - v_h\|_{(L^2(\Omega_N))^3} \;+\; c(\nu_\star)\xi^{\frac{N}{2}}\|(\nu\,B - h^s)\wedge n\|_{(L^2(\Gamma_N))^3}\,,$$

where $c(\nu_\star)$, $c(\nu_0, \nu_\star) > 0$ are constants depending on $\nu_\star$, ν_0 and on the shape of Ω. Therefore we check that there exist constants $C(\nu_\star) > 0$, $C(\nu_0, \nu_\star) > 0$ such that:

$$\|B - B_h\|_{H(\mathrm{div}\,;\,\Omega_N)} \;\le\; C(\nu_0, \nu_\star) \inf_{v_h \in V_h^N} \|B - v_h\|_{H(\mathrm{div}\,;\,\Omega_N)} + C(\nu_\star)\,\xi^{\frac{N}{2}}\,\|(\nu\,B - h^s)\wedge n\|_{(L^2(\Gamma_N))^3}\,. \quad (32)$$

From the same argument that was used in the proof of Theorem 3.1, there exists a constant $c > 0$ independent of N and h such that:

$$\inf_{v_h \in V_h^N} \|B - v_h\|_{H(\mathrm{div}\,;\,\Omega_N)} \;\le\; c\,h\,.$$

To estimate the term $\|(\nu\,B - h^s)\wedge n\|_{(L^2(\Gamma_N))^3}$ of the right hand side of (32), we use, on the one hand, the same constants $R > 0$, $C > 0$ as in Lemma 3.1 in order to check that: $\forall\,|x| > R$, $\|B\wedge n\|^2_{(L^2(\Gamma_N))^3} \;\le\; C\int_{\Gamma_N} \frac{1}{|x|^4}\,dx$. Then, if N is taken as in (16) to satisfy $R > \xi^{N-1}d_\star$, we have:

$$\|B\wedge n\|^2_{(L^2(\Gamma_N))^3} \;\le\; C\,\frac{\mathrm{area}(\Gamma_N)}{(\xi^{N-1}\,d_\star)^4} \;\le\; \frac{C(d_\star)}{\xi^{2N-4}}\,, \quad (33)$$

where $C(d_\star) > 0$ is a constant depending only on C, $d_\star$ and on the shape of Ω. On the other hand, the same arguments are used to estimate $\|h^s\wedge n\|_{(L^2(\Gamma_N))^3}$. Of course, since there exist $R_s > 0$, $C_s > 0$ such that: $\forall\,|x| > R_s$, $|h^s(x)| \;\le\; \frac{C_s}{|x|^2}$, if N is finally taken to ensure

$\min(R, R_s) > \xi^{N-1} d_\star$, it follows that $\|h^s \wedge n\|^2_{(L^2(\Gamma_N))^3} \leq \frac{c(d_\star)}{\xi^{2N-4}}$, with $c(d_\star) > 0$ a constant depending only on C_s, $d_\star$ and on the shape of Ω. Combining together (33) and this last estimate, we get

$$\|(\nu\, B - h^s) \wedge n\|_{(L^2(\Gamma_N))^3} \leq \frac{C(\nu_0, d_\star)}{\xi^{N-2}}\,,$$

with $C(\nu_0, d_\star) > 0$ a constant depending on ν_0, $d_\star$ and on the shape of Ω. The required condition on N is therefore determined from the relation: $\frac{1}{\xi^{\frac{N}{2}-2}} \leq h$, and is given of course by (24).

The asymptotic formula in Theorem 3.2 shows the link between three parameters: the mesh size obtained from the construction of $\mathcal{T}$, the homothetic coefficient ξ chosen for the construction of the first homothetic layer $\mathcal{C}_1$, and the number of homothetic layers N to choose for delimiting the truncated domain Ω_N.

Remark 3.3. The additive hypothesis made on h^s is in accordance with physics. Indeed, h^s is typically created by a current density exciting an inductor and is thus compactly supported; moreover, the decay rate of h^s is natural since it is similar to the one of curl$A$ from (12).

Let us mention that a result similar to Theorem 3.2 can also be derived by using the same arguments, when the infinite mesh is truncated with a Dirichlet boundary condition on the magnetic induction.

3.4 Implementations

Here, we assume that a number of homothetic layers N is chosen and consider the truncated formulations (21) and (23). We describe the implementation of (23) and discuss some numerical algorithms in view of efficient computations. The implementation of (21) is similar to the one of (23).

We call respectively NK, NF, NIF, nf the number of tetrahedra, faces, internal faces and boundary faces resulting from the triangulation $\mathcal{T}$ covering Ω such that: $NF = NIF + nf$. We also denote by NKE, NFE, $NIFE$ the number of tetrahedra, faces, internal faces of the triangulation of one layer $\mathcal{C}_k$, such that: $NFE = NIFE + 2nf$. Of course, each internal edge of $\mathcal{C}_k$ has its vertices on Γ_{k-1} and Γ_k, and following the construction of $\overline{\mathcal{T}}$, there exists a same number nf of faces on the interface $\Gamma_0 \equiv \Gamma$ of Ω and $\mathcal{C}_1$, and on each interface Γ_k of $\mathcal{C}_k$ and $\mathcal{C}_{k+1}$. There exist also a same number $NIFE$ of internal faces and a same number NKE of tetrahedra in each layer $\mathcal{C}_k$.

Let us write, in accordance with (7), a vector field B_h of the space $\mathfrak{B}_h^N$ with the above notations:

$$B_h \;=\; \sum_{f=1}^{NIF} B_h^f u_f + \sum_{k=1}^{N} \sum_{f=1}^{NIFE} B_h^{f,k} u_{f,k} + \sum_{k=0}^{N} \sum_{f=1}^{nf} B_h^{f,\Gamma_k} u_{f,k}\,, \tag{34}$$

where

- u_f, $u_{f,k}$ are the shape functions associated with an internal face f of Ω and with a face f of $\mathcal{C}_k$ respectively. These shape functions are written as in (7);
- B_h^f, $B_h^{f,k}$, B_h^{f,Γ_k} are the scalar unknowns associated with an internal face f of Ω, an internal face f of the layer $\mathcal{C}_k$ and a face f on Γ_k respectively.

With these notations, $u_{f,0}$ is the shape function associated with a face f of Γ and B_h^{f,Γ_0} is the corresponding unknown.

We also write an element ψ_h of the space $\mathcal{Q}_h^N$ as follows:

$$\psi_h \;=\; \sum_{e=1}^{NK} \psi_h^e q_e + \sum_{k=1}^{N} \sum_{e=1}^{NKE} \psi_h^{e,k} q_{e,k}\,, \tag{35}$$

where

- q_e, $q_{e,k}$ are the volume functions associated with a tetrahedron e of Ω and with a tetrahedron e of $\mathcal{C}_k$ respectively;
- ψ_h^e, $\psi_h^{e,k}$ are the scalar unknowns respectively associated with a tetrahedron e of Ω, and a tetrahedron e of $\mathcal{C}_k$.

The variational equations of (23) yield a linear system of finite dimension when the scalar function ν is constant in each tetrahedron. Namely, the discrete system associated with (23) consists of finding (B_h, ψ_h) such that:

$$\begin{pmatrix} M & R^t \\ R & 0 \end{pmatrix} \begin{pmatrix} B_h \\ \psi_h \end{pmatrix} = \begin{pmatrix} s \\ 0 \end{pmatrix}, \tag{36}$$

where we have denoted

$$M = \begin{bmatrix} U & C^t & 0 & 0 & 0 & 0 & \cdots & & 0 \\ C & Z+Z_1 & F^t & G^t & 0 & 0 & \cdot & & 0 \\ 0 & F & L & Y^t & 0 & 0 & \cdot & & 0 \\ 0 & G & Y & A+\xi^{-1}Z_1 & \xi^{-1}F^t & \xi^{-1}G^t & \cdot & & \\ 0 & 0 & 0 & \xi^{-1}F & \xi^{-1}L & \xi^{-1}Y^t & & & \\ 0 & 0 & 0 & \xi^{-1}G & \xi^{-1}Y & \xi^{-1}A+\xi^{-2}Z_1 & & & \\ & & & & & & & & \\ \cdot & & & & & \cdot & & & \\ \cdot & & & & & & \cdot & & 0 \\ \cdot & & & & & & & \cdot & \xi^{-(N-1)}G^t \\ & & & & & & & \cdot & \xi^{-(N-1)}Y^t \\ 0 & 0 & 0 & & & 0 & \xi^{-(N-1)}G & \xi^{-(N-1)}Y & \xi^{-(N-1)}A \end{bmatrix}, \tag{37}$$

with "t" the transpose, and

$$R = \begin{bmatrix} W & E & 0 & 0 & 0 & 0 & 0 & 0 & \cdots & 0 \\ 0 & K & S & P & 0 & 0 & 0 & 0 & \cdot & 0 \\ 0 & 0 & 0 & \xi^{-3}K & \xi^{-3}S & \xi^{-3}P & 0 & 0 & \cdot & 0 \\ & & & & & & & & & \\ \cdot & & & & & \cdot & & & & \\ \cdot & & & & & & \cdot & & & \\ \cdot & & & & & & & \cdot & & \cdot \\ 0 & & & & \cdots & 0 & \xi^{-3(N-2)}K & \xi^{-3(N-2)}S & \xi^{-3(N-2)}P & 0 & 0 \\ 0 & 0 & 0 & & & \cdots & 0 & 0 & \xi^{-3(N-1)}K & \xi^{-3(N-1)}S & \xi^{-3(N-1)}P \end{bmatrix}. \tag{38}$$

The construction of the matrices M and R uses the following homothetic formulæ: $\forall\, k \geq 2$,

$$\int_{\mathcal{C}_k} u_{f,k} \cdot v_{f,k}\, dx = \xi^{-1} \int_{\mathcal{C}_{k-1}} u_{f,k-1} \cdot v_{f,k-1}\, dx\,,$$

$$\int_{\mathcal{C}_k} \mathrm{div} u_{f,k}\, q_{e,k}\, dx = \xi^{-3} \int_{\mathcal{C}_{k-1}} \mathrm{div} u_{f,k-1}\, q_{e,k-1}\, dx\,,$$

where $u_{f,k}$ (as $v_{f,k}$) and $q_{e,k}$ are the shape functions associated respectively with a face f and a tetrahedron e of $\mathcal{C}_k$. The construction of the array s appearing in the right hand side of (36) uses the same arguments as in the construction of M.

In (37), the matrix blocks

$$\begin{bmatrix} U & C^t \\ C & Z \end{bmatrix}, \begin{bmatrix} Z_1 & F^t & G^t \\ F & L & Y^t \\ G & Y & A \end{bmatrix}, \tag{39}$$

correspond to the bilinear forms $(u_h, \eta_h) \in \mathfrak{B}_h^N \times \mathfrak{B}_h^N \longmapsto (\nu\, u_h, \eta_h)_{(L^2(\Omega))^3}$, $(u_h, \eta_h) \in \mathfrak{B}_h^N \times \mathfrak{B}_h^N \longmapsto (\nu\, u_h, \eta_h)_{(L^2(\mathcal{C}_1))^3}$ respectively. With these matrix blocks, we assemble in particular the matrix block associated with the layer $\mathcal{C}_k$:

$$\xi^{-(k-1)} \begin{bmatrix} Z_1 & F^t & G^t \\ F & L & Y^t \\ G & Y & A \end{bmatrix},$$

and therefore the matrix M. Thus, we just need to compute and store the matrix blocks given in (39) in order to get M. We can already mention that the storage of M is easily performed according to the reduced size of the matrix blocks in (39) and to their structure since only non zero terms will have to be kept.

In the same way, in (38), the matrix blocks

$$\begin{bmatrix} W & E \end{bmatrix}, \begin{bmatrix} K & S & P \end{bmatrix}, \tag{40}$$

correspond to the bilinear forms $(u_h, \phi_h) \in \mathfrak{B}_h^N \times \mathcal{Q}_h^N \longmapsto (\operatorname{div} u_h, \phi_h)_{L^2(\Omega)}$, $(u_h, \phi_h) \in \mathfrak{B}_h^N \times \mathcal{Q}_h^N \longmapsto (\operatorname{div} u_h, \phi_h)_{L^2(\mathcal{C}_1)}$ respectively. Also, with these matrix blocks, we assemble in particular the matrix block associated with the layer $\mathcal{C}_k$:

$$\xi^{-3(k-1)} \begin{bmatrix} K & S & P \end{bmatrix},$$

and therefore the matrix R. Again in the same way, as for the matrix M, the storage of R is easily performed, since we just need to compute and store the matrix blocks of reduced size given in (40). Although the dimension of the matrix of system (36), equal to $NT \times NT$ with $NT = NIF + N * NIFE + (N+1) * nf + NK + N * NKE$, can be large, the storage of this matrix is easily performed.

Let us specify that a system similar to (36) is associated with the truncated formulation (21) in the same way. We will retain that the matrix system associated with (21) or with (23) takes into account two parameters: the homothetic coefficient ξ and the number of layers N.

An efficient way to compute (B_h, ψ_h) in (36) consists of using an iterative algorithm according to the size of the system. The matrix M in (36), obtained from a symmetric and positive definite bilinear form, is regular and after eliminating the unknown B_h in (36), we get the matrix equation: $R\, M^{-1}\, R^t\, \psi_h = R\, M^{-1}\, s$. There exist many methods (see e.g. [8], [12]) for solving (36) by using this matrix equation. The Uzawa algorithm [8] associated with the usual Conjugate Gradient method (see e.g. [12]) turns out to be a quite efficient algorithm for solving (36). Namely, applying to (36) the Uzawa algorithm consists algebraically of applying the Conjugate Gradient method to the matrix equation. In such a process, the computation of the inverse of M depends highly on ξ and N, and appears to be the most expensive step in the Uzawa iterations (see also [2] for similar observations). In fact, when ξ is much larger than 1,

the tetrahedra used for the discretization of the first homothetic layer $\mathcal{C}_1$ have an elongated shape and the condition number of M becomes bad. When $\xi \approx 1$, the tetrahedra of $\mathcal{C}_1$ become flat and also, the condition number of M is bad. On the other hand, a disproportion in the coefficients between first lines and last lines of M may create numerical instabilities for large values of N since $\xi > 1$. To avoid this, an idea (see [1], [2]) consists of removing all the powers of ξ in M with the help of a change of variables in (36). Here, we will restrict ourselves to the treatment of (36) with the iterative process combining the Uzawa algorithm with the Conjugate Gradient method (preconditioned by the diagonal of M for computing M^{-1}). This iterative process will allow in particular to overcome the full storage of matrix blocks in (39) and (40).

4. Some Numerical Results

In the first part of this section, we recast a mixed formulation in magnetic induction using boundary elements, in view of a comparison with the numerical results deriving from exponential mesh approximations. Namely, in the last part of this section, the numerical results obtained with the formulations (21) and (23) are described.

4.1 Remarks for the Boundary Element Approximation

The mixed discrete formulation using boundary elements and deriving from (1) − (2) is recalled as follows (see [15]).

For h^s and ν given, find $((B_h, \zeta_h), \psi_h)$ in the space $\mathcal{M}_h \times \Psi_h$ such that:

$$\left\{\begin{array}{lcll} (\nu\, B_h, \eta_h)_{(L^2(\Omega))^3} & + & \nu_0 < \mathcal{L}(\zeta_h), \kappa_h > & + (\operatorname{div} \eta_h, \psi_h)_{L^2(\Omega)} \quad = \\ (h^s, \eta_h)_{(L^2(\Omega))^3} & + & < n \wedge h^s, \kappa_h > & \forall\, (\eta_h, \kappa_h) \in \mathcal{M}_h\,, \\ (\operatorname{div} B_h, \phi_h)_{L^2(\Omega)} & = & 0 & \forall\, \phi_h \in \Psi_h\,. \end{array}\right. \tag{41}$$

The vector field n represents the unit normal to Γ, inwardly directed to Ω. We have denoted by $\mathcal{L}$ the boundary operator such that: $\forall\ \zeta \in TH^{-\frac{1}{2}}(\text{curl};\ \Gamma) = \{p \in (H^{-\frac{1}{2}}(\Gamma))^3\,;\ \operatorname{curl}_\Gamma p \in H^{-\frac{1}{2}}(\Gamma),\ p \cdot n = 0\}$, $\mathcal{L}(\zeta) = n \wedge \operatorname{curl} A$ with $\operatorname{curl}(\operatorname{curl} A) = 0$ in Ω', $\operatorname{div} A = 0$ in Ω', and $n \wedge (A \wedge n) = \zeta$ on Γ. Using the same notations and the same triangulation as $\mathcal{T}$ (with the mesh size $h := h_{\mathcal{T}}$) introduced in subsection 3.1, we have set:

$$\begin{array}{rcl} \mathcal{D}_h & = & \{B_h \in H(\operatorname{div}\,;\Omega)\,;\ B_h|_K \in D^1 \quad \forall\, K \in \mathcal{T}\}\,, \\ \mathcal{C}_h & = & \{\zeta_h\,;\ \zeta_h|_T \in R^1_\Gamma \quad \forall\, T \in \mathcal{T} \cap \Gamma\}\,,\ R^1_\Gamma = \{q = n \wedge p\,;\ p \in D^1|_\Gamma\}\,, \\ \mathcal{M}_h & = & \{(B_h, \zeta_h) \in \mathcal{D}_h \times \mathcal{C}_h\,;\ B_h \cdot n = \operatorname{curl}_\Gamma \zeta_h \ \text{ on } \Gamma\}\,, \\ \Psi_h & = & \{\psi_h \in L^2(\Omega)\,;\ \psi_h|_K \in P_0 \ \forall\, K \in \mathcal{T}\}\,. \end{array}$$

Here $< .\,,\,. >$ is the duality product between $\{p \in (H^{-\frac{1}{2}}(\Gamma))^3\,;\ \operatorname{div}_\Gamma p \in H^{-\frac{1}{2}}(\Gamma),\ p \cdot n = 0\}$ and $TH^{-\frac{1}{2}}(\text{curl};\ \Gamma)$; $\operatorname{curl}_\Gamma$ and $\operatorname{div}_\Gamma$ are the surface curl and surface divergence. As it is noted in [15], the solution (B_h, ζ_h) determined with (41) is unique and the vector field B_h is in accordance with (1) − (2). Let us mention that the mixed formulation (8), proposed in this work, appears as a variant of (41) considered in the whole three-dimensional space. We refer to [15] for details concerning (41) and its continuous version. More precisely, we refer to the discretization of the boundary operator $\mathcal{L}$ and to the treatment of the relation $B_h \cdot n = \operatorname{curl}_\Gamma \zeta_h$ (expressed in [15] as the *matching condition* on Γ of the magnetic induction). The matrix corresponding to the boundary term $< \mathcal{L}(\zeta_h), \kappa_h >$ is a full square matrix block of dimension $ne \times ne$. When the number ne of edges on Γ increases, the size of this full matrix block increases and its memory storage requirement becomes more important. In [15], the matrix system associated with (41) is solved with the Uzawa algorithm. In this procedure, the

Conjugate Gradient method is used for computing the inverse of the matrix associated with the bilinear form $((u_h, \zeta_h), (\eta_h, \kappa_h)) \in \mathcal{M}_h \times \mathcal{M}_h \longmapsto (\nu\, u_h, \eta_h)_{(L^2(\Omega))^3} + \nu_0 < \mathcal{L}(\zeta_h), \kappa_h >$.

Some numerical results obtained with (41) will be compared below (see subsection 4.3) with those deriving from exponential mesh computations.

4.2 Some Considerations

In the case where h^s is a constant vector field, with Ω spherical and homogeneous, it is known (see [10]) that the analytic solution of $(1)-(2)$ is given in Ω by the formula: $B = \frac{3}{(1+2\,\nu_r)\,\nu_0} h^s$ where $\nu_r = \frac{\nu}{\nu_0}$ ($\nu_0 = 1/4\pi 10^{-7}$ MKSA) is the relative magnetic reluctance. As in [15], we consider $h^s = H_0\, e_z$ where the unit vector e_z is oriented following Oz with H_0 a real constant. We distinguish here the cases $\nu_r = 0.9$, 0.85 and give some characteristics of the balls $\mathcal{B}_1, \mathcal{B}_2$ (which represent Ω) in the following table:

	NK	NIF	NE	nf	ne	h_p
$\mathcal{B}_1$	160	280	254	80	120	0.85104
$\mathcal{B}_2$	1280	2400	1748	320	480	0.60982

For a ball $\mathcal{B}_p$, the mesh size is denoted h_p and NK, NIF, NE are respectively the number of tetrahedra, internal faces and edges. Also, we denote by nf, ne the number of faces and edges on the boundary of $\mathcal{B}_p$. These balls have the same radius, taken as equal to one meter. We set

$$div_{L^2(\mathcal{B}_p)} = \|\mathrm{div}\, B_h\|_{L^2(\mathcal{B}_p)}\,,\ err_{L^2(\mathcal{B}_p)} = \frac{\|B - B_h\|_{(L^2(\mathcal{B}_p))^3}}{\|B\|_{(L^2(\mathcal{B}_p))^3}}\,.$$

We mentioned in subsection 3.1 that the layers used in the discretization of the exterior domain Ω' have the same triangulation. Here, as the domain Ω is a ball $\mathcal{B}_p$ ($p = 1, 2$), each layer is represented by a spherical wreath $\mathcal{C}_{\mathcal{B}_p}$ with few characteristics given in the following table:

	NKE	$NIFE$	NEE	nfe
$\mathcal{C}_{\mathcal{B}_1}$	240	400	402	160
$\mathcal{C}_{\mathcal{B}_2}$	960	1600	1602	640

Each $\mathcal{C}_{\mathcal{B}_p}$ is built from the ball $\mathcal{B}_p$. We denote respectively by NKE, $NIFE$, NEE the number of tetrahedra, internal faces, and edges of $\mathcal{C}_{\mathcal{B}_p}$. Also, $nfe = 2\,nf$ is the number of faces on the boundary of $\mathcal{C}_{\mathcal{B}_p}$. The mesh size of $\mathcal{C}_{\mathcal{B}_p}$ depends here on the homothetic coefficient ξ.

4.3 Exponential Mesh Computations

We first consider the matrix system associated with the formulation (21) in order to compute the vector field B_h satisfying $(1)-(2)$ in a truncated domain where a Dirichlet boundary condition is enforced. This matrix system is solved with the Uzawa algorithm using the Conjugate Gradient method, where the stopping parameters (on the residues) are ϵ_{uz} and ϵ_{cg} respectively.

The numerical results presented below are described with respect to ξ and N. We will observe that the computations with Dirichlet boundary conditions do always appreciably better than those with boundary conditions of Neumann type and that in addition, the relative error err_{L^2} can be improved by loading the layers until a limiting case (see Figure 3.).

Figures $2.-3.$ present some results on the relative error err_{L^2} when $\mathcal{B}_1$ is considered, $\nu_r = 0.9$ and $\epsilon_{uz} = \epsilon_{cg} = 10^{-6}$. On these figures, we also mark the value $err_{L^2(\mathcal{B}_1)} = 0.3280106$E-01 which is obtained from boundary element computations (see (41)) with the same choice of parameters ν_r, ϵ_{uz} and ϵ_{cg}.

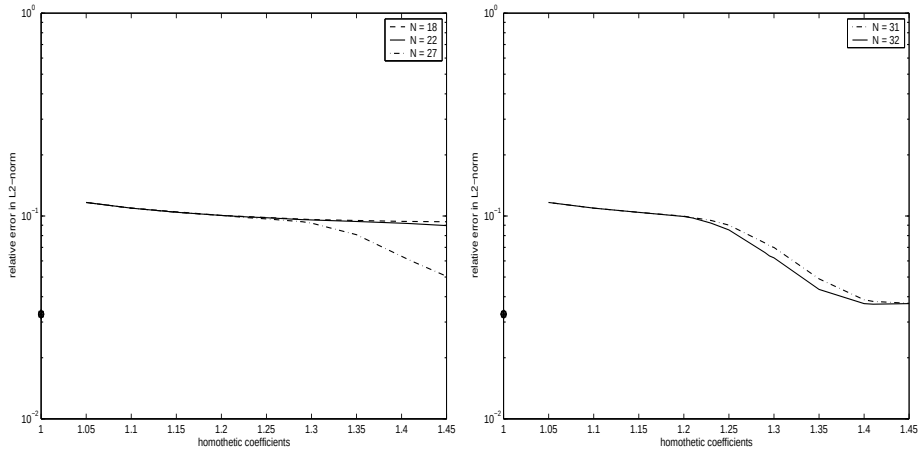

Figure 2: $err_{L^2(\mathcal{B}_1)}$ with $\nu_r = 0.9$; at left $N = 18, 22, 27$ and at right $N = 31, 32$.

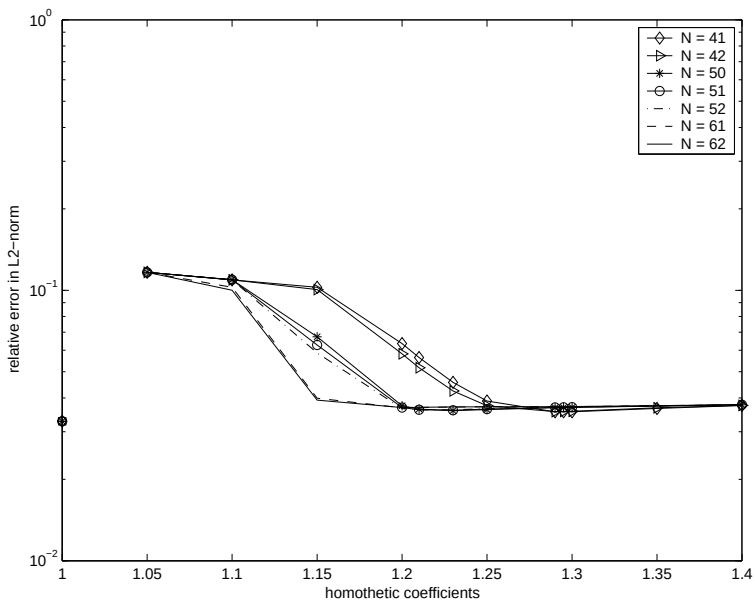

Figure 3: $err_{L^2(\mathcal{B}_1)}$ with $\nu_r = 0.9$.

The relative error depends on the two parameters ξ and N. We observe that for $\xi \approx 1.29$ and $N = 41$ we already obtain good results. However, this is not the case for other values of ξ and N (see e.g. Figure 2.). The following table contains some values of $err_{L^2(\mathcal{B}_1)}$ and of $div_{L^2(\mathcal{B}_1)}$ obtained under the same considerations.

N	41	41	41
ξ	1.29	1.295	1.3
$err_{L^2(\mathcal{B}_1)}$	0.3553820E-01	0.3554119E-01	0.3556726E-01
$div_{L^2(\mathcal{B}_1)}$	0.2630796E-04	0.2661785E-04	0.2679507E-04

Figure 4. presents some results on the relative error when $\mathcal{B}_1$ is considered, $\nu_r = 0.85$ and $\epsilon_{uz} = \epsilon_{cg} = 10^{-6}$. The value $err_{L^2(\mathcal{B}_1)} = 0.4775338$E-01 obtained with (41) for the same choice of parameters ν_r, ϵ_{uz} and ϵ_{cg} is marked on this figure.

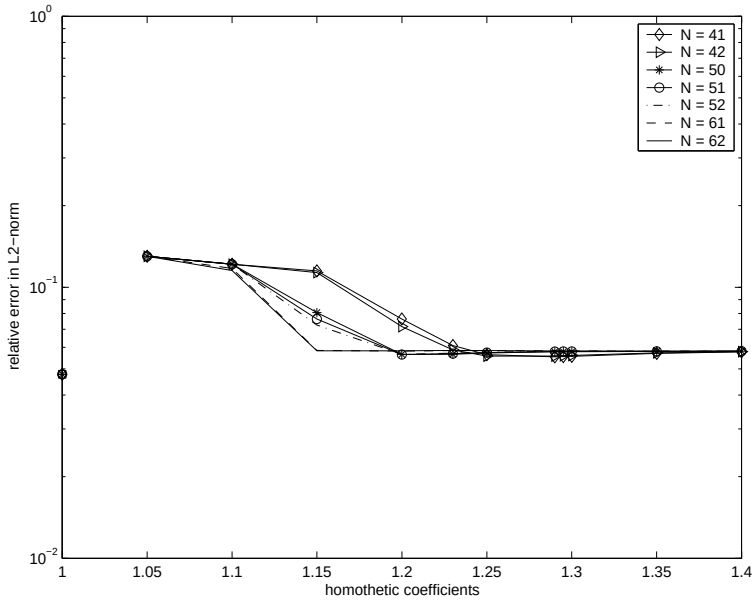

Figure 4: $err_{L^2(\mathcal{B}_1)}$ with $\nu_r = 0.85$.

The relative error also depends on the magnetic reluctance ν_r. Let us mention on the other hand that the influence of the stopping criteria can improve the results. More precisely, the divergence-free constraint on the magnetic induction is well satisfied when small values for ϵ_{uz} are considered (see e.g. the following table where $\epsilon_{cg} = 10^{-6}$ and $\epsilon_{uz} = 10^{-8}$).

N	41	41	41
ξ	1.29	1.295	1.3
ν_r	0.9	0.9	0.9
$div_{L^2(\mathcal{B}_1)}$	0.6257244E-05	0.7634007E-05	0.8235050E-05

In Figures 5. – 6., we present some results when (21) is considered with $\mathcal{B}_2$, $\nu_r = 0.9$, $\epsilon_{uz} = \epsilon_{cg} = 10^{-6}$. The value $err_{L^2(\mathcal{B}_2)} = 0.1366710$E-01 obtained from (41) in that case is marked on Figure 5. Also, some comparisons of the results between $\mathcal{B}_1$ and $\mathcal{B}_2$ are performed.

We already mention that, as with $\mathcal{B}_1$, the relative error depends also on ξ, N and ν_r. It is observed (see Figure 6.) on the other hand that the optimal values of ξ and N differ on $\mathcal{B}_1$ and $\mathcal{B}_2$.

The numerical results described above allow us to conclude that the computation of the magnetic induction with (21) is appreciably as accurate as with (41).

We consider here the formulation (23) and recall that it allows to compute the vector field B_h satisfying (1) – (2) in a truncated domain where a boundary condition of Neumann type is enforced. Some results obtained from (23), by taking $\epsilon_{uz} = \epsilon_{cg} = 10^{-6}$, are compared in Figure 7. with those of (41) and (21). It is observed from numerical simulations with (23) that the

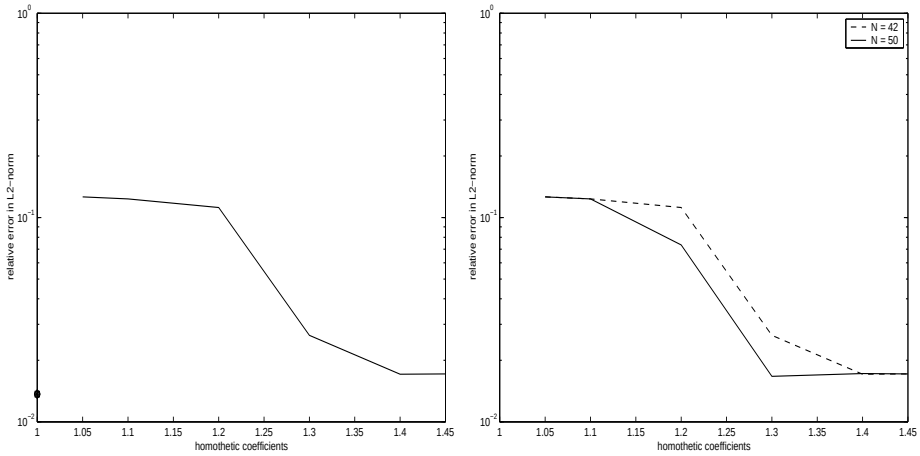

Figure 5: $err_{L^2(\mathcal{B}_2)}$ with $\nu_r = 0.9$; at left $N = 42$ and at right $N = 42, 50$.

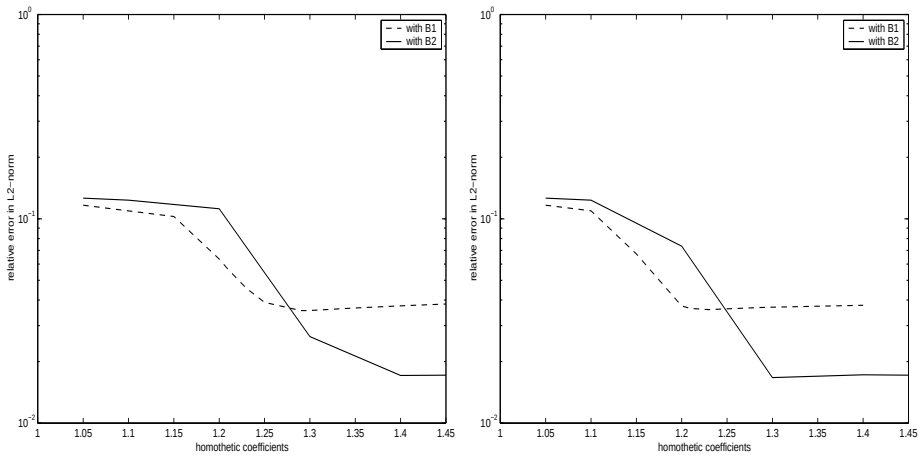

Figure 6: Comparison between $\mathcal{B}_1$ (– –) and $\mathcal{B}_2$ (—) of err_{L^2} with $\nu_r = 0.9$; at left $N = 42$, and at right $N = 50$.

relative error err_{L^2} (as well as div_{L^2}) preserves the same behavior with respect to ξ, N and ν_r as in the case of simulations with (21).

The obtained results show that the computation with (23) is slightly less accurate than that with (21), or that with (41). Also, as indicated for example in Figure 8., the CPU time needed in the computation with (23) is more important than the one needed in the computation with (21). This suggests that the use of a truncated domain, with a Dirichlet boundary condition enforced, is more suitable for the computation of the considered magnetic induction.

From these numerical simulations (carried out on an SGI Origin 3200 of "CRI of Orsay"), it has been globally observed that the CPU time needed in exponential mesh computations is excessively expensive when compared with the CPU time ($<<$ 1800 s. with $\mathcal{B}_1$ for example) obtained from (41).

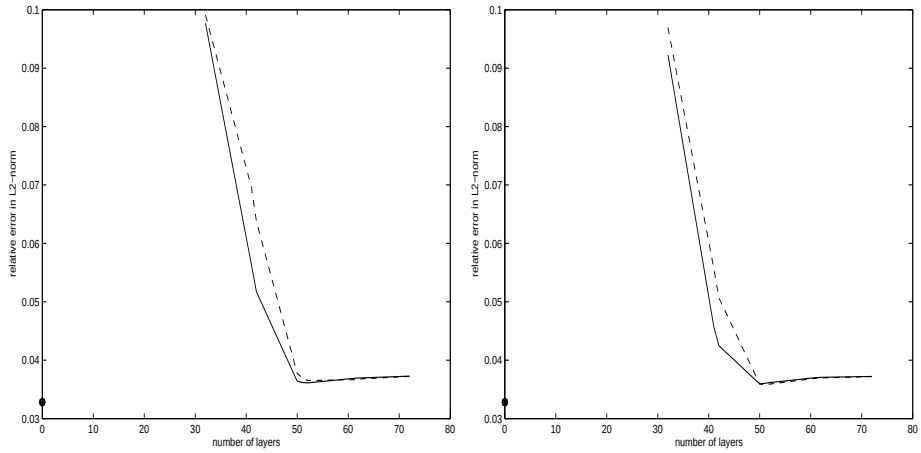

Figure 7: Comparison of $err_{L^2(\mathcal{B}_1)}$ with $\nu_r = 0.9$, boundary condition of Neumann type (– –) and Dirichlet boundary condition (—). At left $\xi = 1.21$, and $\xi = 1.23$ at right.

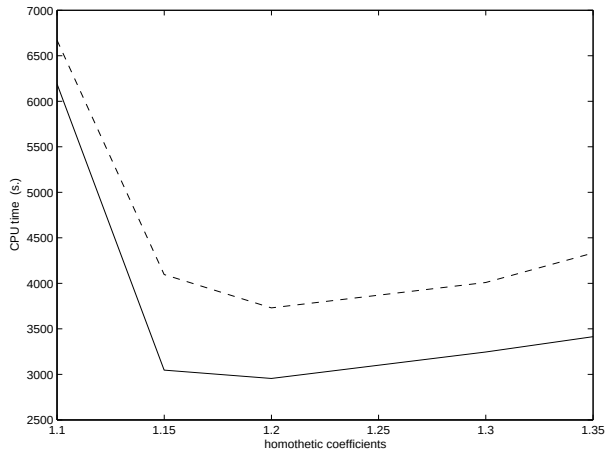

Figure 8: Comparison of the CPU time with $\mathcal{B}_1$, $N = 42$, $\nu_r = 0.9$, $\epsilon_{uz} = \epsilon_{cg} = 10^{-6}$, boundary condition of Neumann type (– –) and Dirichlet boundary condition (—).

5. Conclusions

A numerical method based on the use of an exponential mesh, in association with face and volume elements, has been described for computing a magnetic induction. Dirichlet boundary conditions and those of Neumann type have been considered for the truncations of the exponential mesh. It has been observed that the computations of the magnetic induction with Dirichlet boundary conditions do always appreciably better than those with boundary conditions of Neumann type and are on the other hand appreciably as accurate as with a boundary element computation. Although, the exponential mesh method yields an easy implementation with a saving storage, and can be considered as an alternative to the boundary element method, the CPU time required in the exponential mesh computations is a drawback. In fact, this CPU time is excessively expensive in comparison to the one needed with the boundary element computation of the considered magnetic induction.

Acknowledgements. The author would like to thank the referees for their useful suggestions. Their constructive remarks have improved the presentation of some parts of this work.

References

[1] F. Alouges, Computation of the demagnetizing potential in micromagnetics using a coupled finite and infinite elements method, *ESAIM Control Optim. Calc. Var.*, **6** (2001), 629–647.

[2] F. Alouges, J. Laminie & S.M. Mefire, Exponential meshes and three-dimensional computation of a magnetic field, *Numer. Meth. for Partial Differential Equations*, **19** (2003), 595–637.

[3] I. Babuska, The finite element method with Lagrangian multipliers, *Numer. Math.*, **20** (1973), 179-192.

[4] A. Bayliss, M. Gunzburger & E. Turkel, Boundary conditions for the numerical solution of elliptic equations in exterior regions, *SIAM J. Appl. Math.*, **42** (1982), 430-451.

[5] A. Bossavit, Electromagnétisme, en Vue de la Modélisation, Springer-Verlag, Paris, 1993.

[6] A. Bossavit, The computation of eddy-currents, in dimension 3, by using mixed finite elements and boundary elements in association, *Mathl. Comput. Modelling*, **15** (1991), 33-42.

[7] F. Brezzi, On the existence, uniqueness and approximation of saddle point problems arising from Lagrangian multipliers, *RAIRO*, 8 (1974), 129-151.

[8] F. Brezzi & M. Fortin, Mixed and Hybrid Finite Element Method, Springer-Verlag, New-York, 1991.

[9] R. Dautray & J.-L. Lions, Analyse Mathématique et Calcul Numérique pour les Sciences et les Techniques, Tome 6, Masson, Paris, 1988.

[10] E. Durand, Magnétostatique, Masson, Paris, 1968.

[11] G. Duvaut & J.-L. Lions, Les Inéquations en Mécanique et en Physique, Dunod, Paris, 1972.

[12] V. Girault & P. A. Raviart, Finite Element Methods for Navier-Stokes Equations, Springer-Verlag, New-York, 1986.

[13] D. Givoli, Nonreflecting boundary conditions, *Comput. Phys.*, **94** (1991), 1–29.

[14] C.I. Goldstein, The finite element method with nonuniform mesh sizes for unbounded domains, *Math. Comp.*, **36** (1981), 387–404.

[15] S.M. Mefire, Mixed finite element and boundary element approximation in 3D magnetostatics for computation of the magnetic induction, *Appl. Math. Comput.*, **125** (2002), 399–421.

[16] S.A. Nazarov & M. Specovius-Neugebauer, Approximation of exterior problems, Optimal conditions for the Laplacian, *Analysis*, **16** (1996), 305–324.

[17] J.-C. Nédélec, Mixed finite elements in $\mathbb{R}^3$, *Numer. Math.*, **35** (1980), 315–341.

[18] J.-C. Nédélec, Elements finis mixtes incompressibles pour l'équation de Stokes dans $\mathbb{R}^3$, *Numer. Math.*, **39** (1982), 97–112.

[19] P.A. Raviart & J.-M. Thomas, A Mixed Finite Element Method for 2nd Order Elliptic Problems, *in Mathematical aspects of finite element methods*, Springer Verlag, Rome 1975; *Lecture Notes in Math.*, 606 (1975).

[20] L.-A. Ying, Infinite Element Methods, Peking University Press, Beijing, 1995.